UNCLASSIFIED

SECURITY CLASSIFICATION OF THIS PAGE

(2)

AD-A215 284

REPORT DOCUMENTATION PAGE

1a REPORT SECURITY CLASSIFICATION: UNCLASSIFIED	1b RESTRICTIVE MARKINGS
2a SECURITY CLASSIFICATION AUTHORITY	3 DISTRIBUTION/AVAILABILITY OF REPORT: APPROVED FOR PUBLIC RELEASE DISTRIBUTION IS UNLIMITED
2b DECLASSIFICATION/DOWNGRADING SCHEDULE	
4 PERFORMING ORGANIZATION REPORT NUMBER(S)	5 MONITORING ORGANIZATION REPORT NUMBER(S): AFOSR-TR- 89-1580
6a NAME OF PERFORMING ORGANIZATION: Princeton University; 6b OFFICE SYMBOL (If applicable)	7a NAME OF MONITORING ORGANIZATION: AFOSR/NA
6c ADDRESS (City, State and ZIP Code): Princeton, N.J. 08544	7b ADDRESS (City, State and ZIP Code): BUILDING 410, BOLLING AFB, DC 20332-6448
8a NAME OF FUNDING/SPONSORING ORGANIZATION: AFOSR/NA; 8b OFFICE SYMBOL (If applicable): NA	9 PROCUREMENT INSTRUMENT IDENTIFICATION NUMBER: AFOSR Grant 88-0120
8c ADDRESS (City, State and ZIP Code): BUILDING 410 - BOLLING AFB, DC 20332-6448	10 SOURCE OF FUNDING NOS: PROGRAM ELEMENT NO 61102F; PROJECT NO 2307; TASK NO. A2; WORK UNIT NO.
11 TITLE (Include Security Classification): (U) Physical Models for Supersonic Turbulent Boundary Layer Structure	
12. PERSONAL AUTHOR(S): Alexander J. Smits	
13a TYPE OF REPORT: FINAL; 13b TIME COVERED: FROM 2/15/88 TO 6/14/89	14 DATE OF REPORT (Yr, Mo, Day): 1989 October 17; 15. PAGE COUNT: 30
16 SUPPLEMENTARY NOTATION	
17 COSATI CODES: FIELD / GROUP / SUB GR	18 SUBJECT TERMS (Continue on reverse if necessary and identify by block number): Boundary Layer, Supersonic Turbulence

19. ABSTRACT (Continue on reverse if necessary and identify by block number)

see reverse side

20. DISTRIBUTION/AVAILABILITY OF ABSTRACT: UNCLASSIFIED/UNLIMITED ☒ SAME AS RPT ☐ DTIC USERS ☐	21 ABSTRACT SECURITY CLASSIFICATION: UNCLASSIFIED
22a NAME OF RESPONSIBLE INDIVIDUAL: JAMES M MCMICHAEL	22b TELEPHONE NUMBER (Include Area Code): 202-767-4935; 22c OFFICE SYMBOL: AFOSR/NA

DD FORM 1473, 83 APR EDITION OF 1 JAN 73 IS OBSOLETE

UNCLASSIFIED

SECURITY CLASSIFICATION OF THIS PAGE

19.

This report is the final report for AFOSR Grant 88-0120, monitored by Dr. J. McMichael. An experimental program was carried out to study the detailed structure of supersonic turbulent boundary layers. The experiments were designed to elucidate physical models and mechanisms that are particular to compressible turbulence, such as the effects of compressibility on the nature of the large-scale motions, the scaling laws for high Reynolds number supersonic turbulent flows, direct compressibility effects that cause the exchange of turbulence energy among the vorticity, entropy and sound modes, and the transport of heat and momentum by compressible turbulent motions.

In Section 2. a detailed description of the completed work is given, including a description of the new optical experimental tools developed in conjunction with Prof. Miles. Appendix A contains a list of the publications acknowledging this grant, and Appendix B gives a list of the personnel involved with the work, including the degrees awarded during the period of the grant.

FINAL REPORT

to the
Air Force Office of Scientific Research
Attn: Dr. J. McMichael

Covering the Period 2/15/88 through 6/14/89

"PHYSICAL MODELS FOR SUPERSONIC TURBULENT BOUNDARY LAYER STRUCTURE"

AFOSR Grant 88-0120

By

A. J. Smits
Gas Dynamics Laboratory
Department of Mechanical and Aerospace Engineering
Princeton University
Princeton, N. J. 08544

TABLE OF CONTENTS

1. INTRODUCTION

This report is the final report for AFOSR Grant 88-0120, monitored by Dr. J. McMichael. An experimental program was carried out to study the detailed structure of supersonic turbulent boundary layers. The experiments were designed to elucidate physical models and mechanisms that are particular to compressible turbulence, such as the effects of compressibility on the nature of the large-scale motions, the scaling laws for high Reynolds number supersonic turbulent flows, direct compressibility effects that cause the exchange of turbulence energy among the vorticity, entropy and sound modes, and the transport of heat and momentum by compressible turbulent motions.

In Section 2, a detailed description of the completed work is given, including a description of the new optical experimental tools developed in conjunction with Prof. Miles. Appendix A contains a list of the publications acknowledging this grant, and Appendix B gives a list of the personnel involved with the work, including the degrees awarded during the period of the grant.

2. DETAILED DESCRIPTION OF COMPLETED WORK

Here, we review our work on the study of the structure of supersonic turbulent boundary layers in zero and adverse pressure gradients, and the flow of a turbulent boundary layer over curved surfaces. A description of the new optical techniques developed by Prof. Miles is also given.

2.1 The structure of supersonic turbulent boundary layers

A considerable amount of new insight into the turbulence structure of supersonic turbulent boundary layers has been obtained, through the detailed study of representative boundary layer flows. The data include measurements of $\langle u' \rangle$, $\langle (\rho u)' \rangle$, $\langle v' \rangle$ and $-\overline{\rho u' v'}$, and they have been reported in great detail in the recent AGARDograph by Fernholz, Smits, Dussauge and Finley (1988). In addition, measurements of higher order moments have been made, and spectral data, probability density distributions, and correlations have also been obtained in all cases. In this respect, these data sets are the most complete data sets for zero and adverse pressure gradient supersonic boundary layers currently available.

During the grant period, studies of a zero pressure gradient, and an

adverse pressure gradient flow on a flat plate were completed (Fernando (1988), Spina (1988)), as well as a study of the behavior of a supersonic turbulent boundary layer on curved surfaces (Donovan (1989)). This work was used to assess the significance of variable density on the structure of high speed turbulent boundary layers. For the purpose of comparison with the subsonic case we used the results from Alving (1988) because of the wide variety of data obtained in that flow. The flow conditions for these cases, and some others, are summarized in Table I. Because of the experimental conditions of these tests, and the lack of high-quality, detailed data from other sources, it is not always possible to make a clear distinction between Mach and Reynolds number effects.

According to Morkovin (1962), the dynamics of compressible turbulent shear layers follow the incompressible pattern closely, as long as the fluctuauating Mach number remains small. In supersonic Flows 1 and 2, the freestream Mach number is in the range where Morkovin's hypothesis should apply over most of the boundary layer thickness. The Mach number gradient near the wall, however, is very high (for example, in Flow 1 the sonic line is located at approximately $y = 0.005\delta = 0.13mm = 75\ \nu_w/u_\tau$), and it may be expected that the fluctuating Mach number can exceed unity in the region of maximum turbulence production, and Morkovin's hypothesis may break down in the near-wall region.

The simplest comparison between the turbulence behavior in subsonic and supersonic boundary layers is to compare the distributions of $\langle u' \rangle$. When normalized by u_τ ($= \sqrt{\tau_w/\rho_w}$), the distributions appear to show a strong Mach number effect (see, for example Schlichting 1968, p. 659). However, if the results for Mach numbers less than 5 are normalized by a velocity scale derived using the wall stress and the local density ($= \sqrt{\tau_w/\rho}$), as suggested by Morkovin, the Mach number dependence is no longer evident. At a Mach number of 6.7, however, Owen et al. found that this transformation did not seem to collapse the data, indicating that hypersonic flow may display strong compressibility effects. It is also known that the flatness profile in supersonic flows is more constant than in the corresponding subsonic case (see figure 2). One definition of intermittency is $I = (3/\text{Flatness})$, where $\text{Flatness} = \overline{u'^4}/(\overline{u'^2})^2$, and the results imply that the intermittency profile is fuller in supersonic flows. In contrast, the Rayleigh scattering density

Subsonic flow	Supersonic flow 1	Supersonic flow 2	Supersonic flow 3
M_∞	0.1	2.9	2.97	6.7
U_{ref}	31 m/s	565 m/s	594 m/s	1110 m/s
C_f	.00283	.00114	.00166	.00080
R_θ	5000	80,000	15000	8500
δ	19.3 mm	28 mm	12 mm	33 mm

Table 1. Experimental conditions for the supersonic boundary layers investigated by Spina (1988) and Fernando (1988) (Flow 1), Robinson (1986) (Flow 2), and Owen et al. (1975) (Flow 3), and the subsonic boundary layer investigated by Alving (1988).

field flow visualization by Smith at Princeton (private communication) reveals that the boundary layer has a very similar appearance to that seen in subsonic flows (see figure 3), and it may be possible that the flatness profiles of $(\rho u)'$ do not give an accurate picture of the intermittency. Recent measurements of the intermittency function from the $(\rho u)'$ signal by Selig (1988) seems to support this idea. What is even more interesting is that the shear correlation coefficient R_{uv} $(= -\overline{u'v'}/\langle u'\rangle\langle v'\rangle)$ is different (figure 4). The subsonic data reveal a higher correlation across the boundary layer with a nearly constant value of 0.45 for $0 < y/\delta < 0.8$, while the supersonic correlation decreases steadily as y/δ increases. Differences were also observed in the distribution of the structure parameter $a_1 = -\overline{u'v'}/q^2$ (not shown). In these same studies, however, Fernando and Alving found similar anisotropy ratios, suggesting that the difference in character of the R_{uv} distribution is caused by a change in the shear stress, that is, the organized motions, not by a change in u' or v' alone. These changes are clearly evident in the joint probability density distributions of u' (or $(\rho u)'$) and v', shown in figure 5. The contributions to $-\overline{u'v'}$ are organized differently; as a basis for comparison, it may be seen that the major axes of

these approximately elliptical distributions are aligned more closely with the horizontal axis when the flow is supersonic. A wide variety of two-point space-time correlation data is available, including mass-flux $(\rho u)'$ (or velocity u') correlations in the streamwise, normal, and spanwise directions (x, y, and z, respectively). To begin the discussion of the results, consider the time records of $(\rho u)'$ obtained in the zero pressure gradient boundary layer from three hot wires (figure 6). The signals exhibit a very similar character, indicating the passage of organized motions of a scale larger than the separation distance between the top and bottom wires. The space-time correlations for one supersonic and one subsonic flow are shown in figure 7. For both cases, the peak values of the correlations are quite high, reaching a maximum of 0.65 near the middle of the boundary layer. The correlation frictions for the supersonic boundary layer are considerably narrower than for subsonic layer. Furthermore, the dimensionless delay time corresponding to the peak of the space-time correlation, τ_{max}, decreases from 0.4 (= 20 $\pm$ 0.5μs) at the floor to nearly zero at the edge of the boundary layer.

The high peak level of the correlation and the non-zero value of the time delay imply that both wires are detecting the same "disturbance", and that one wire is detecting it before the other. Since the time shift was applied to the upper wire, the peak at negative time delay means that the upper wire detects the disturbance first, that is, the disturbance leans downstream. Accordingly, an angle θ can be defined for this "front" by using the value of τ_{max} along with the wire separation distance, ξ, and the local convection velocity. That is,

$$\theta = \tan^{-1}\left[\frac{\xi}{U_c \tau_{max}}\right]$$

The angle θ may be called an "average structure angle," in that it is associated with an average large-scale motion. Figures 8 and 9 show that the structure angle depends on the distance between the two measurement points, and that the distribution for supersonic flow is different from that in subsonic flow. In the supersonic case for small values of ξ (ξ/δ = 0.09 ,say), the structure angle is approximately constant at a value between 45° and 50° for $0.2 < y/\delta < 0.8$. For $\xi/\delta \geq 0.2$, the structure angle becomes

insensitive to variation in the separation distance, and it varies from about 40^o at $y/\delta = 0.2$ to about 60^o at $y/\delta = 0.8$. In the subsonic case, however, small values of ξ give larger values of θ, and large values of ξ gives smaller values of θ than those observed in the supersonic case. For example, Alving found that for $\xi/\delta = 0.1$, the structure angle was approximately at a value of 60^o for $0.2 < y/\delta < 0.8$, whereas for $\xi/\delta \geq 0.2$, θ varied from about $20\text{-}30^o$ to about 50^o over the same interval in y. Note that the uncertainty in the convection velocity will not affect these results significantly: when $\theta = 45^o$, 0% error in U_c leads to an error in θ of only $2\text{-}3^o$. These results help to explain the differences seen in the correlation functions (figure 7). Since the average large-scale structure is more upright in a supersonic boundary layer, the space-time correlation is apt to fall off at shorter time delays since the extent of the structures in the mean flow direction will be smaller.

Using the same upstream flow conditions used by Spina and Smits for the zero pressure gradient layer discussed above, Donovan and Smits (1987) investigated the mean structure angle distribution following a short region of concave surface curvature using two different flow models: one which turns the flow through 8^o with a radius of curvature of 1270 mm ($\delta/R = .022$), and the other turns the flow 16^o with $\delta/R = .08$. Fernando and Smits (1987) made similar measurements on a flat plate following a short region of adverse pressure gradient. In that case, the pressure gradient was generated by a contoured plate, designed so that the pressure distribution matched that of the 8^o model using by Donovan and Smits. The general shape of the distribution remained the same as in the zero pressure gradient case. However, there appeared to be a small increase in the structure angle after each of the three perturbations. Furthermore, the structure angle after the stronger curvature was slightly higher than after the weaker curvature. Donovan and Smits suggested that the perturbation rate was too rapid in the stronger curvature model to allow readjustment of the large-scale motions, and thus the angle of inclination is affected. It appears that the same preliminary conclusion can be drawn for all three of the flow perturbations, since they all exhibit the same trend.

While the present study traversed two "detection probes" through the boundary layer at a fixed separation distance (small compared to δ), most

other measurements of this kind have used one detection probe fixed at the wall (a hot wire, a shear stress gauge, or some similar device) and another probe which was traversed through the boundary layer, thereby varying the separation distance. The fixed separation method used here results in a typical mean structure angle of 45° in supersonic flow and about 30° in subsonic flow. While the variable separation method seems to give a lower characteristic value; in supersonic flow Robinson (1986) found 30° and in incompressible flows Brown and Thomas (1977) found 18°, whereas Rajagopalan and Antonia (1979) found 12.5°, and Robinson (1985) found 16°. The advantage of the present method is that the slope of the structure is determined locally, instead of being inferred from a large-scale measurement.

A superposition of peak time delays on the "mean structure shape" was used to produce iso-correlation contours for the supersonic case using $\xi = 0.09\delta$ and 0.30δ (figure 10). The "mean structure shape", the solid curve drawn through the center of the contours, was constructed from an extrapolation of the mean structure angle from one measurement location to the next (with the first location supplying the appropriate inclination from the origin). The peak of the cross-correlation at each mean wire position was then shifted so that it was coincident with the curve delineating the mean structure shape. The contours give a good indication of the extent of the field around the identified structure. The same mean structural characteristics are evident in all of the contours, as well as those determined by Robinson. Similar contour plots were derived for the subsonic boundary layer studied by Alving and they are given in figure 11. The differences in mean structure angle that exist between supersonic and subsonic flows (figures 8 and 9) are readily apparent in figures 10 and 11, as are the much greater streamwise extent of the large-scale structures in the subsonic boundary layer.

Donovan (1989) has studied the space-time correlations in the supersonic boundary layer flow downstream of the short region of concave surface curvature described earlier. He observed a significant elongation of the average structure in the streamwise direction, consistent with the distortion that would be observed if the large scale motion can be represented by a horseshoe vortex model.

In addition to the measurements made at two points separated in the

direction normal to the wall, measurements were taken at a variety of spanwise spacings in both the supersonic and subsonic cases. The space-time correlation for a spanwise spacing of 0.09δ is shown in figure 12 for several locations across the supersonic boundary layer. The corresponding results for the subsonic boundary layer are given in figure 13. The peak values are somewhat lower than in the supersonic case, although the correlations are much broader. In both cases, however, the character and strength of the correlations is similar to those found for the vertical separations, except that the peak occurs at zero time delay in this case. Since the correlation between wires spaced 0.09δ apart is similar for both the spanwise and vertical alignments, a similarity of the structures is suggested in the y- and z-directions for small distances in both cases. As determined from the peak values of the correlation functions, it appears that the spanwise scales are slightly smaller than the vertical scales.

A comparison of the length scales based entirely upon the peak values of the correlations is not conclusive, however. Therefore, the transverse scales were further explored with the aid of iso-correlation contours which give the behavior of the entire correlation curve, not just the peak value. The space-time correlations were reflected about $\xi = 0$ for each y-position (this is valid since the spanwise correlations are symmetric), and iso-correlation contours were drawn from the resulting surfaces (figures 14 and 15). As with the vertical correlations, the time delay was normalized by outer-layer variables, and by Taylor's hypothesis can be interpreted as a streamwise distance. The plots then give (pseudo) x-z cross-sections of the boundary layer at three different y-locations. What is very striking is that the spanwise extent of the large-scale motions in subsonic and supersonic flows are almost identical (and in good agreement with the results of Kovasznay et al. 1970), whereas the streamwise scale differs by a factor of about two. In addition, the spanwise scale of the detected structures increases away from the wall. Since the overall size of the structures increases with y/δ this behavior is not surprising. The spanwise scale of the detected organized structures should therefore increase as we move farther from the wall.

All the measurements presented here indicate that despite broad

similarities, the turbulence structure of supersonic and subsonic boundary layers display significant differences. Some of these differences, such as the change in the flatness profile, have been observed in previous studies, and are now relatively well known. Structure parameters have not been widely studied in supersonic flows, however, and the new measurements presented here indicate that strong differences exist. For example, the length scales derived from space-time correlations indicate that the spanwise scales are almost identical but that the streamwise scales in the subsonic flow are about half the size of those in supersonic flow. The large-scale structures in the subsonic boundary layer also appear to move slightly slower, and lean more towards the wall, than those observed in supersonic flows, and their shear stress content is distributed differently among the four quadrants. All these observations suggest that there may be fundamental differences between the structure of subsonic and supersonic boundary layers. It is possible that the density gradients in a supersonic shear layer affect the large scale structure, and that there exists a damping effect of Mach number on the turbulent motions which may be important even for turbulence away from the wall. In some sense it would not be surprising to find differences between compressible and incompressible boundary layers since the vorticity transport equation describes the transport of vorticity per unit mass, rather than the absolute vorticity, and there is a contribution from the non-barotropic term. Density gradients must therefore affect the vorticity dynamics to some extent, and the extent of this influence will vary with Mach number.

2.2 New Optical Techniques For Investigating Compressible Turbulent Flows

The image of the shock wave/boundary layer interaction shown in figure 16 was made possible by using a high-power, far ultraviolet excimer laser in conjunction with a high-sensitivity, far ultraviolet camera. By focusing the laser into a thin sheet of light and passing it through the wind tunnel, cross-sectional images of the air density can be recorded by direct Rayleigh scattering. Due to the ω^4 dependence of the Rayleigh scattering cross section, operation in the far-UV produces a signal which is approximately 60 times that in the visible. Even though the excitation is near resonant transitions in oxygen, the Rayleigh scattering cross section of air in this

region is virtually independent of laser frequency and molecular temperature (Miles et al. 1988a). As a consequence, the collected light level is a direct measure of the air density. Illumination is with an argon-fluoride laser operating in the vicinity of .193 microns with a pulse duration of 10 nsec, so the cross-sectional image is frozen in time. This diagnostic technique may be used together with vibrational tagging of oxygen molecules to yield, simultaneously, an instantaneous velocity profile. This method for generating velocity profiles combines Raman Excitation plus Laser-Induced Electronic Fluorescence (RELIEF) and some recent results for experiments in free shear layers were reported by Miles et al. (1988b). Examples of lines which have been marked before and after the Mach disk of an underexpanded free jet are shown in figure 17. The lines in both cases were marked 2 μsec before the image was taken, so the line deformation is a quantitative measure of the velocity profile. Rayleigh scattering was simultaneously recorded to give the density cross section. The Rayleigh scattering technique has already given the first detailed, quantitative, two-dimensional picture of the turbulent structure of a supersonic boundary layer (see below). The RELIEF method is currently being extended to boundary layer measurements to obtain simultaneous time-lines which will complement the density cross sections presented here.

A small Mach 3 supersonic wind tunnel was constructed and fitted with UV transmitting quartz windows so that the laser sheet could be passed through the flow field. The high-sensitivity camera observed the scattering at 90° and images could be recorded up to the camera framing rate of 30 Hz. At the point of interrogation, the Reynolds number, based on the boundary layer momentum thickness, was 15,000. The tunnel was operated as a blow down facility and exhausted into atmospheric pressure. An example of a single cross-sectional image taken normal to the boundary layer in the streamwise direction is shown in figure 18 (the flow is the same as that shown in figure 3: the flow is from right to left). Regions of high density are bright and regions of low density are dark. There is some scattering from the wall which causes a bright region at the very bottom of the image. The scale, from top to bottom, is 7 mm and the resolution is on the order of several hundred microns. The boundary layer thickness is approximately 5 mm. Figure 19 is a false color rendition of this same boundary layer image with

the scattering from the bottom trimmed off. Cross-sectional images parallel to the boundary layer (plan views) can also be recorded, and figure 20 is a typical plan view image taken 3 mm above the wall.

In a qualitative fashion, these images show that there are well-defined individual structures located in the boundary layer. The dark areas of the image represent low density regions characteristic of high temperatures. The bright areas are the high densities found in the free stream. Intermittent penetration of freestream fluid deep into the boundary layer is clearly visible in figure 18. The plan view (figure 20) gives an even better appreciation of the intermittency at a given height in the boundary layer. From many such images a statistical picture of the intermittency can be generated.

Furthermore, since the brightness of the image is a quantitative measure of the density of the gas, these images may be examined to give probability density distributions across the flow and at different height locations within the boundary layer. Density correlations can also be developed to give a quantitative measure of the scale of the turbulent structures. Figure 21 is the probability density distribution function taken from figure 20. Even though it comes from a single frame, this probability density distribution of the density fluctuations is similar to the probability density distribution of the mass-flux fluctuations by Hayakawa et al. (1984) in a similar flow, giving indirect support for the Strong Reynolds Analogy.

In addition, we can now contrast this statistical result with an instantaneous picture of the density distribution. It is interesting to note from figure 19, for example, that the boundary layer appears to consist of large regions of relatively uniform low density, separated from the high density region by a rather thin buffer zone.

In summary, we have obtained instantaneous two-dimensional density cross sections in supersonic flow fields using a new nonintrusive flow diagnostic method. These images have already provided new insight into the structure of the boundary layers, and have generated statistical information on the density fluctuations. These represent the first direct measurements of the density fluctuations obtained in a supersonic turbulent boundary layer. When combined with the flow marking technique, we will have the first opportunity to directly observe the coupling between vorticity and density.

APPENDIX A: Publications Acknowledging Grant 88-0120

REFEREED PUBLICATIONS

Fernholz, H.H., Smits, A.J., Dussauge, J.-P. and P. J. Finley, (Eds.), "A Survey of Measurements and Measuring Techniques in Rapidly Distorted Compressible Turbulent Boundary Layers," NATO-Advisory Group for Aerospace Research and Development AGARDograph, #315, 1989.

Smits, A. J., Alving, A. E., Smith, R. W., Spina, E. F., Fernando, E. M. and Donovan, J. F., "A Comparison of the Turbulence Structure of Subsonic and Supersonic Boundary Layers", to be presented at the Eleventh Symposium on Turbulence, University of Missouri-Rolla, Rolla, Missouri, October 17-19, 1988. Accepted for publication, The Physics of Fluids, 1989.

Fernando, E. M. and Smits, A. J., "A Supersonic Turbulent Boundary Layer in an Adverse Pressure Gradient". Accepted for publication, Journal of Fluid Mechanics, 1989.

Alving, A. E., Smits, A. J. and Watmuff, J. H., "Turbulent Boundary Layer Relaxation from Convex Curvature", Accepted for publication, Journal of Fluid Mechanics, 1989.

Baskaran, V., Smits, A. J. and Joubert, P. N., "A Turbulent Flow over a Curved Hill. Part II. Effects of Streamline Curvature." Submitted for publication, Journal of Fluid Mechanics, 1989.

PAPERS (publications appearing in conference proceedings -acceptance decided by review of abstract)

Fernando, E. M. and Smits, A. J., "The Kinematics of Simple Vortex Loop Arrays," AIAA Paper #88-3657, First National Fluid Dynamics Conference, Cincinatti, Ohio, July 24-28, 1988.

Smits, A. J., "The Structure of Supersonic Turbulent Boundary Layers: What We Know and What We Think We Know", International Workshop on the Physics of Compressible Turbulent Mixing, Princeton, N. J., October 24-27, 1988.

Fernando, E. M., Donovan, J. F., Smith, D. R. and Smits, A. J., "Conventional Skin Friction Measurement Techniques for Strongly Perturbed Supersonic Turbulent Boundary Layers", AIAA Paper 89-1861, AIAA 20th Fluid Dynamics Conference, Buffalo, New York, June 12-14, 1989.

Smits, A. J., "Physical Models For Supersonic Turbulent Boundary Layer Structure", presented at AFOSR Contractors Meeting on Turbulence Research, USC Los Angeles, June 1988.

Smits, A. J., "Lecture Series on Turbulence with Compressibility", NASA Ames/Stanford University Center for Turbulence Research, July 1988.

APPENDIX B: Personnel and Degrees Granted

a) Personnel Information

The Gasdynamics Laboratory at Princeton University is staffed by:

Prof. Alexander J. Smits (Principal Investigator)

Prof. Seymour M. Bogdonoff (Director, Gas Dynamics Laboratory)

Dr. Kamal Podar (Full-time Research Staff Member)

In addition to the Research Staff, the Laboratory is staffed on a full time basis by two technical specialists and on a part-time basis by a computer specialist.

The activities are supported by 7 research students, all of whom are pursuing Ph.D. studies. Their names are: J. Goldstein, W. Konrad, C. McGinley, J. Poggie, D. Smith, R. Smith and M. Zagarolla. All except two of these students are U. S. Citizens.

During the period of the subject grant, 5 students supported by the grant received the Ph.D. degree. They were Amy Alving (currently at the Technical University of Berlin), Eric Spina (Assistant Professor, Syracuse University), Emerick Fernando (Flow Research), John Donovan (McDonnell-Douglas, St. Louis), and Mike Smith (NASA Langley Research Center).

REFERENCES

Alving, A. E. 1988 "Boundary layer relaxation from convex curvature," Ph.D. Thesis, Princeton Univ., Princeton, NJ.

Blackwelder, R. and Kaplan, R. E. 1976 "On the wall structure of the turbulent boundary layer," J. Fluid Mech. 76,89.

Brown, G. L. and Thomas, A. S. W., [1977], Large structure in a turbulent boundary layer, Physics of Fluids, Vol. 20(10), p. 243.

Deckker, B. E. L. [1980], Boundary layer on a shock tube wall and at a leading edge using schlieren, Second International Symposium on Flow Visualization, Ruhr-Universitat Bochum, West Germany. Ed. W. Merzkirch, Hemisphere, p. 413.

Deckker, B. E. L. and Weekes, M. E. [1976], The unsteady boundary layer in a shock tube, Proc. I. Mech. Eng., Vol. 190, p. 287.

Dolling, D. S. and Murphy, M. T. (1983), "Unsteadiness of the Separation Shock Wave in a Supersonic Compression Ramp Flowfield," AIAA Journal, Vol. 21, pp. 1628-1634.

Donovan, J. F. and Smits, A. J. [1987], A preliminary investigation of large-scale organized motions in a supersonic turbulent boundary layer on a curved surface, AIAA Paper 87-1285.

Dussauge, J. P. and Gaviglio, J. [1981], Bulk dilatation effects on Reynolds stress in the rapid expansion of a turbulent boundary layer at supersonic speed, Proc.Third Symposium on Turbulent Shear Flows, Univ. Cal., Davis.

Dussauge, J. P. and Gaviglio, J. 1987 "The rapid expansion of a supersonic turbulent flow: role of bulk dilatation, "J. Fluid Mech. 174, p. 81.

Fernando, E. M. 1988 "The effects of an adverse pressure gradient on a flat plate, supersonic, turbulent boundary layer," Ph.D. Thesis, Princeton Univ., Princeton, NJ.

Fernando, E. M. and Smits, A. J. [1987], The effects of an adverse pressure gradient on the behavior of a supersonic turbulent boundary layer, AIAA Paper 87-1286.

Fernando, E. M., Spina, E. F., Donovan, J. F. and Smits, A. J. [1987], Detection of large-scale organized motions in a turbulent boundary layer, Sixth Symposium on Turbulent Shear Flows, Toulouse, France.

Fernholz, H. H. and Finley, P. J. 1980 "A critical commentary of compressible turbulent boundary layer data," AGARDograph No. 253.

Head, M. R. and Bandyopadhyay, P. [1981], New aspects of turbulent boundary-layer structure, Journal of Fluid Mechanics, Vol. 107, p. 297.

Hayakawa, K., Smits, A. J. and Bogdonoff, S. M. (1984), "Hot-Wire Investigation of an Unseparated Shock-Wave/Turbulent Boundary-Layer Interaction," AIAA Journal 22, pg. 579.

Horstman, C. C., Settles, G. S., Vas, I. E., Bogdonoff, S. M. and Hung, S. M. (1977), "Reynolds Number Effects on Shock Wave Turbulent Boundary Layer Interactions," AIAA Journal, Vol. 15, pp. 1152-1158.

James, C. S. (1958), Observations of turbulent-burst geometry and growth in supersonic flow, NASA TN 4235.

Johansson, A. V. and Alfredson, p. H. [1982], On the structure of turbulent channel flow, Journal of Fluid Mechanics, Vol. 122, p. 295.

Karniadakis, G. E., Mikic, B. B. and Patera, A. T. (1988), "Minimum Dissipation Transport Enhancement by Flow Destabilization: Reynolds' Analogy Revisited," J. Fluid Mech., 192:365.

Kistler, A. L. 1959 "Fluctuation measurements in a supersonic turbulent boundary layer," Phys. Fluids 2, 290.

Kovasznay, L. S. G., Kibens, V. and Blackwelder, R. F. 1970 "Large-scale motion in the intermittent region of a turbulent boundary layer," J. Fluid Mech. 41, 283.

Lu, L. J. and Smit, C. R. (1985), "Image Processing of Hydrogen Bubble Flow Visualization for Determination of Turbulence Statistics and Bursting Characteristics," Expts. in Fluids, 3:349.

Miles, R., Connors, J., Howard, P., Markovitz, E. and Roth, G. (1988a), "Proposed Single-Pulse, Two-Dimensional Temperature and Density Measurements of Oxygen and Air," Optics Letters 13, pg. 195.

Miles, R., Connors, J., Markovitz, E., Howard, P. and Roth, G. (1988b), "Instantaneous Supersonic Velocity Profiles in an Underexpanded Jet by Oxygen Flow Tagging," (Accepted for publication in Physics of Fluids).

Moin, P. and Kim, J. [1985], The structure of the vorticity field in turbulent channel flow. Part 1 - analysis of instantaneous fields and statistical correlations, Journal of Fluid Mechanics, Vol. 155, p. 441.

Morkovin, M. V. 1962 "Effects of compressibility on turbulent flows," Int. Symp. on the Mechanics of Turbulence 367. C.N.R.S., Paris.

Nosenchuck, D. M. and Lynch, M. K. (1986), "Three-dimensional Flow Visualizations Using Laser-Sheet Scanning," In Proc. AGARD Conf. on Aerodynamics and Related Hydrodynamics Studies Using Water Facilities, pg. 18.1.

Owen, F. K. and Horstman, C. C. [1981], Turbulent measurements in an equilibrium hypersonic boundary layer, AIAA Paper 74-93.

Owen, F. K., Horstman, C.C. and Kussoy, M. I. 1975 "Mean and fluctuating flow measurements of a fully developed, non-adiabatic hypersonic boundary layer," J. Fluid Mech. 70, 393.

Perry, A. E. and Chong, M. S. [1982], On the mechanism of wall turbulence. Journal of Fluid Mechanics, Vol. 119, pp. 173-217.

Rajagopalan, S. and Antonia, R. A. [1979], Some properties of the large structure in a fully developed turbulent duct flow, Physics of Fluids, Vol. 22(4), p. 614.

Robinson, S. K. [1985], Instantaneous velocity profile measurements in a turbulent boundary layer, Chem.Eng. Communications, Vol. 43, p. 347.

Robinson, S. K. [1986], Space-time correlation measurements in a compressible turbulent boundary layer, AIAA Paper 86-1130.

Russell, G. and Miles, R. B. (1987), "Display and Perception of Three-Dimensional Space Filling Data", Applied Optics 26: 973.

Sabadell, L. A., Watmuff, J. H. and Smits, A. J. (1989), "Modification of Turbulence Structure by a Drag-Reducing Surfactant Solution," in preparation.

Selig, M. S., Andreopoulos, J., Muck, K. C., Dussauge, J. P. and Smits, A. J. (1989), "Turbulence Structure in a Shock Wave/Turbulent Boundary Layer Interaction," to be published in AIAA Journal, January.

Settles, G. S., Vas, I. E. and Bogdonoff, S. M. (1976), Details of a Shock-Separated Turbulent Boundary Layer at a Compression Corner," AIAA Journal, Vol. 14, pp. 1709-1715.

Smits, A. J. and Muck, K. C. [1986], Experimental study of three shock wave/turbulent boundary layer interactions. Journal of Fluid Mechanics, Vol. 182.

Smith, C. R. [1984], A synthesized model of near-wall behavior in turbulent boundary layers, Proceedings of Eighth Symposium on Turbulence, (Ed. G. K. Patterson and J. L. Zakin), Department of Chemical Engineering, University of Missouri-Rolla).

Smith, M. W., Kumar, V., Smits, A. J. and Miles, R. B. (1989), "The Structure of Supersonic Turbulent Boundary Layers as Revealed by Line Profiles and Density Cross Sections," to be presented, Seventh Symposium on Turbulent Shear Flows, Stanford University, Stanford, CA.

Smith, M. W. and Smits, A. J. 1988 "Cinematic visualization of coherent density structures in a supersonic turbulent boundary layer," AIAA Paper 88-500.

Smits, A. J., Alving, A. E., Smith, R. W., Spina, E. F., Fernando, E. M. and Donovan, J F. (1988), "A Comparison of the Turbulence Structure of Subsonic and Supersonic Boundary Layers," Proc. Eleventh Symp. on Turbulence, Univ. Missouri-Rolla, Rolla, Missouri.

Smits, A. J., Hayakawa, K. and Muck, K. C. [1983], "Constant-temperature hot-wire anemometer practice in supersonic flows. Part I - The normal wire, Experiments in Fluids, Springer-Verlag.

Smits, A. J., Muck, K. C. and Hayakawa, K. 1983 "Constant temperature hot-wire anemometry practice in supersonic flows, Part I: The normal wire," Experiments in Fluids 1, 83.

Spalart, P. R. (1988), "Direct Simulation of a Turbulent Boundary Layer up to Re_θ = 1410," J. Fluid Mech. 187: 61.

Spina, E. F. 1988 "Organized Structures in a Supersonic Turbulent Boundary Layer" Ph. D. Thesis, Princeton Univ., Princeton, NJ.

Spina, E. F. and Smits, A. J., [1986] "Organized structures in a supersonic turbulent boundary layer", Princeton University, Dept. of Mechanical and Aerospace Engineering, Report #1736.

Spina, E. F. and Smits, A. J. (1987), "Organized Structures in a Compressible Turbulent Boundary Layer," Journal of Fluid Mechanics, 182:85-109.

Thomas, A. S. W. and Bull, M. K. [1983], On the role of wall-pressure fluctuations in deterministic motions in the turbulent boundary layer, Journal of Fluid Mechanics, Vol. 128, p. 283.

Tran, T. T. 1987 "An experimental investigation of unsteadiness in swept shock wave/turbulent boundary layer interactions," Ph.D. Thesis, Princeton Univ., Princeton, NJ.

van Driest, E. R. 1951 "Turbulent boundary layer in compressible fluids," Journal of

Van Dyke, M. [1982], An Album of Fluid Motion, The Parabolic Press, Stanford, CA.Aeronautical Sciences 128, 283.

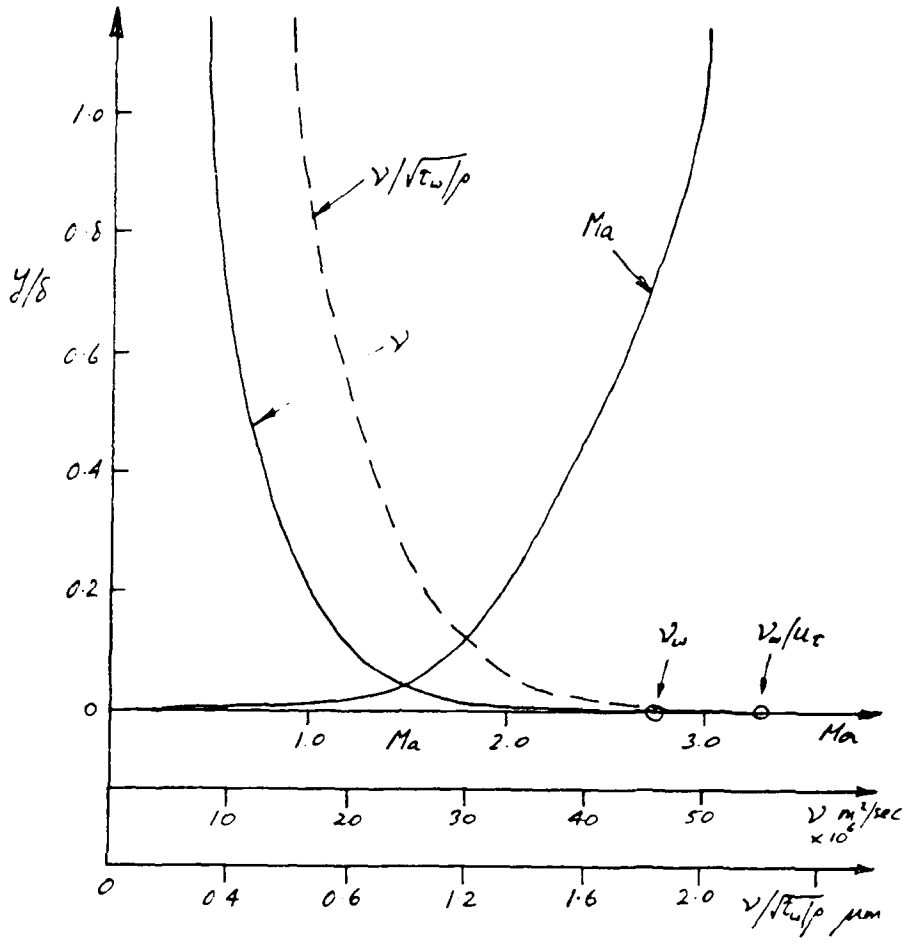

Fig. 1. Distribution of Ma, ν, $\nu/\sqrt{\tau\omega/\rho}$ in compressible turbulent boundary layer with freestream Mach number of 2.9, δ = 26 mm, and R_θ = 80,000 (outer layer variable).

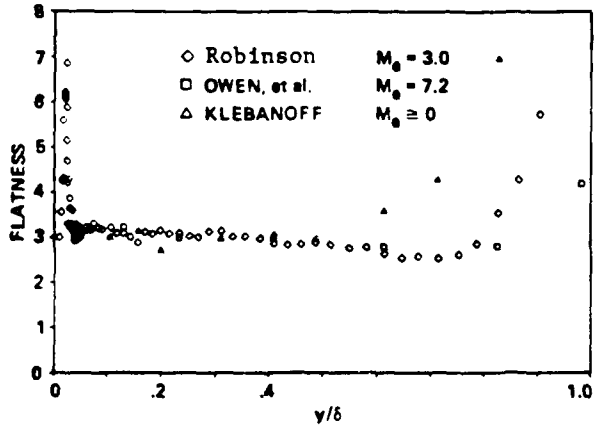

Fig. 2. Comparison of the flatness profiles for the streamwise fluctuations from supersonic (Spina 1988) and subsonic (Alving 1988) turbulent boundary layers.

Fig. 3 Density cross-section of a Mach 2.5 boundary layer. Flow is from right to left.

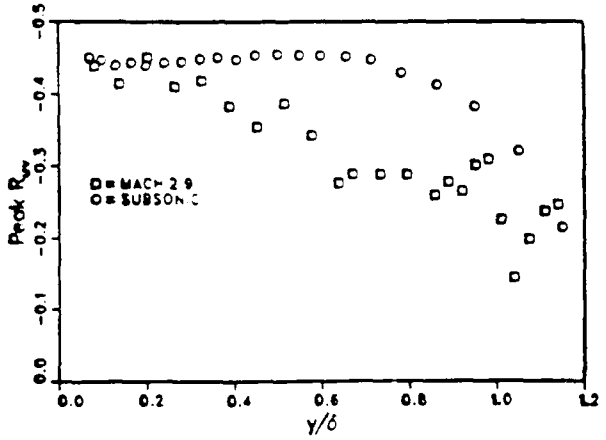

Fig. 4 Comparison of the shear correlation coefficient ($R_{uv} = \overline{u'v'}/\langle u'\rangle\langle v'\rangle$) in supersonic (Fernando 1988) and subsonic (Alving 1988) turbulent boundary layers.

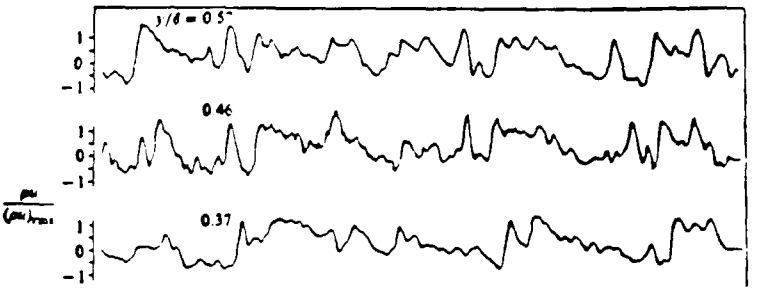

Fig. 6. Three simultaneously measured, instantaneous mass-flux signals (Flow 1, Spina and Smits 1987).

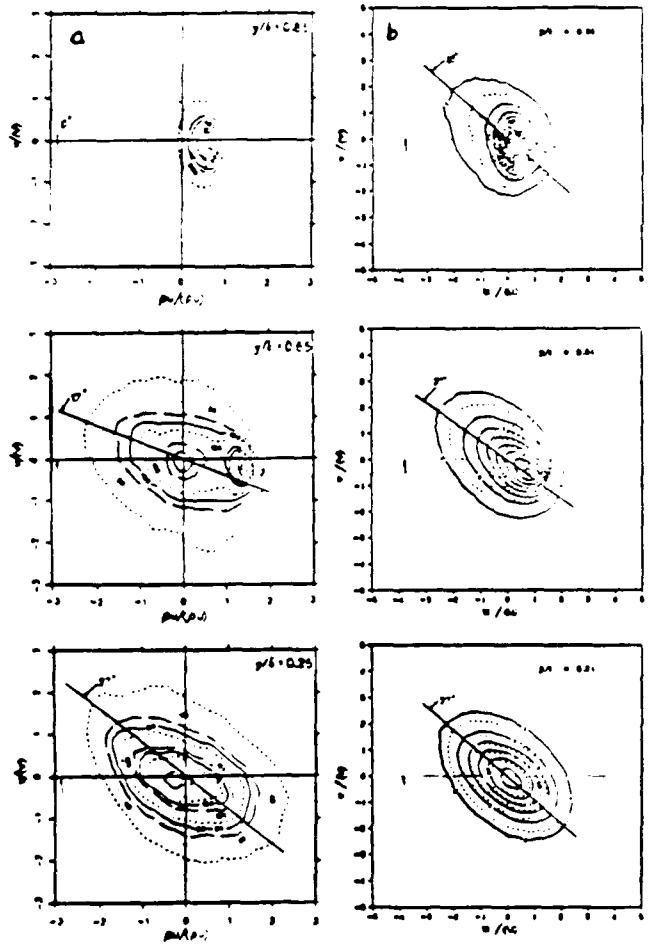

Fig. 5. Probability density function for (a) $\overline{(\rho u)'v'}$ from Fernando (1988), and (b) $\overline{u'v'}$ from Alving (1988).

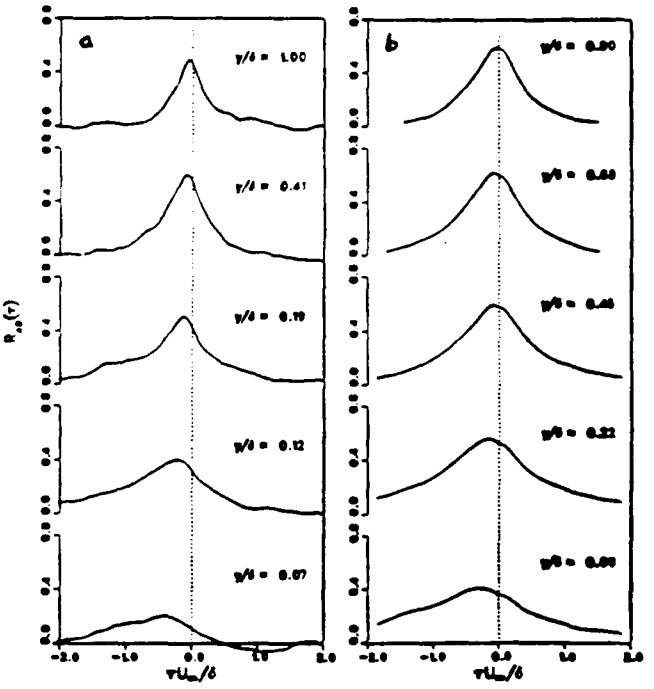

Fig. 7(a) Cross-correlation measurements in the supersonic boundary layer, $\xi/\delta_{99} = 0.09$. From Spina (1988).

Fig. 7(b) Cross-correlation at several positions in the subsonic boundary layer, $\xi/\delta_{99} = 0.10$. From Alving (1988).

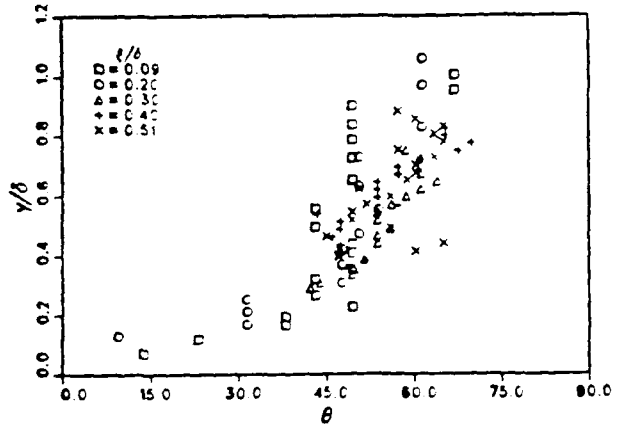

Fig. 8. Large-scale structure angle in the supersonic boundary layer for different wire separation distances (from Spina 1988).

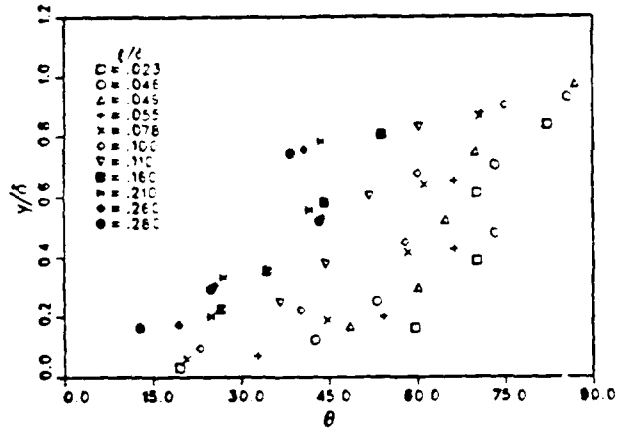

Fig. 9. Large-scale structure angle in the subsonic boundary layer for different wire separation distances (from Alving 1988).

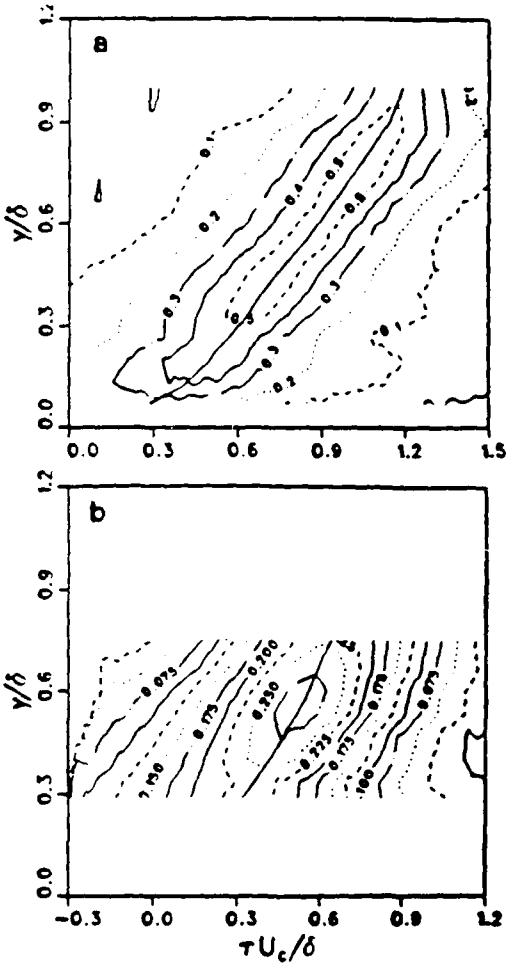

Fig. 10 Equi-value space-time correlation contours from vertically separated mass-flux signals in a supersonic boundary layer: a) ξ = 0.09δ, b) ξ = 0.30δ (from Spina 1988).

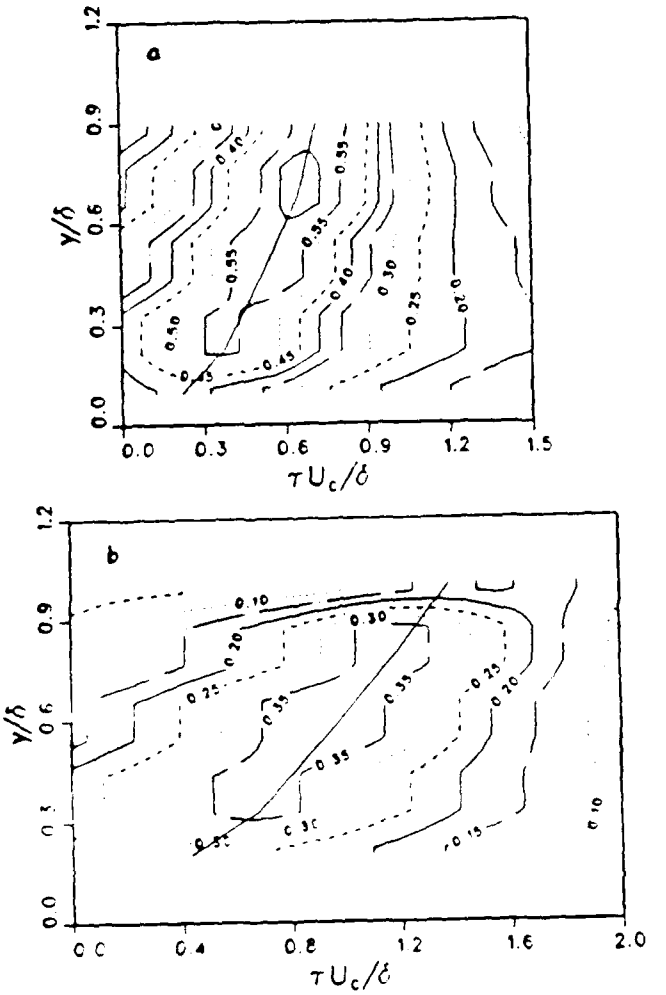

Fig. 11 Equi-value space-time correlation contours from vertically separated velocity signals in the subsonic boundary layer studied by Alving (a) ξ = 0.10, (b) ξ = 0.21, (c) ξ = 0.29.

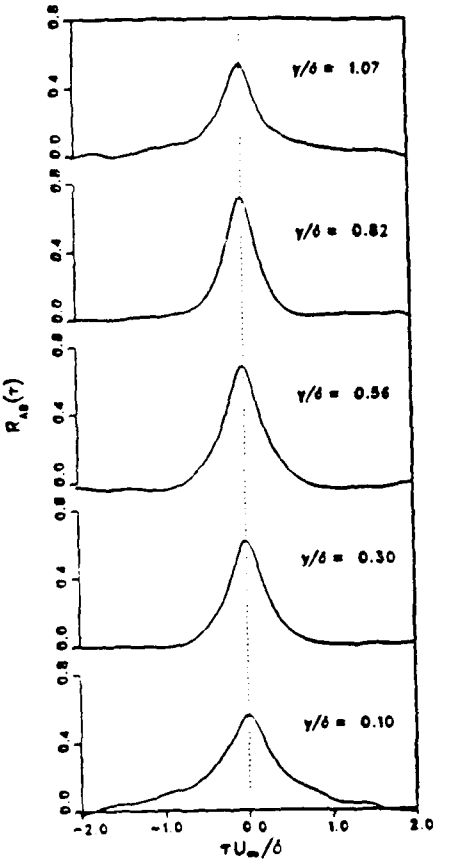

Fig. 12 Space-time correlation between spanwise separated mass-flux signals for several locations in a supersonic boundary layer; ξ = 0.09δ (Spina 1988).

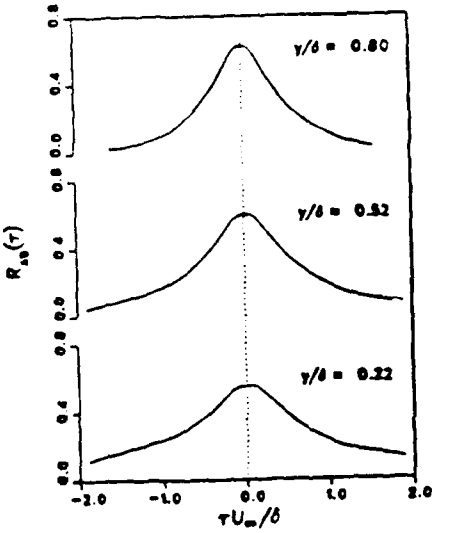

Fig 13 Space-time correlation between spanwise separated velocity signals for several locations in the subsonic boundary layer studied by Alving; ξ = 0.09δ.

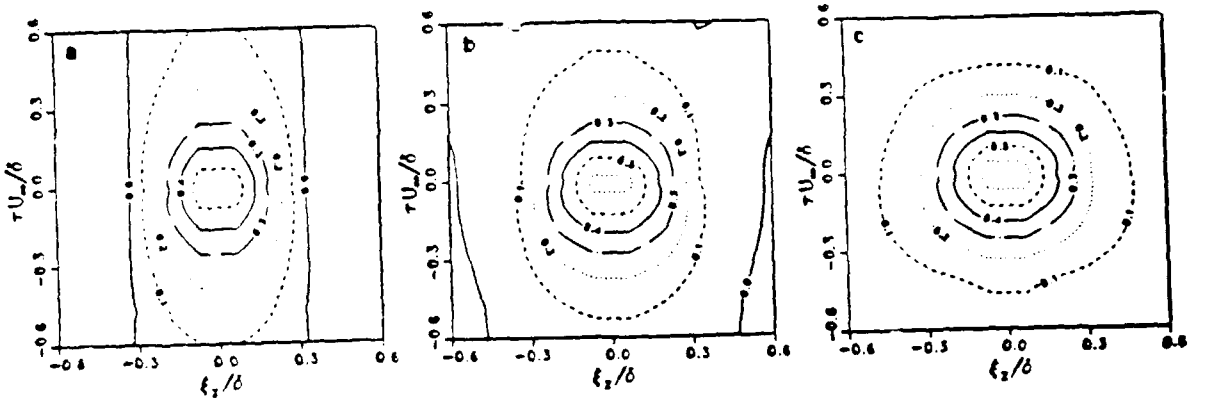

Fig. 14 Equi-value space-time correlation contours from spanwise separated mass-flux signals in the supersonic boundary layer a) $y/\delta = 0.20$, b) $y/\delta = 0.51$, c) $y/\delta = 0.82$ (Spina 1988).

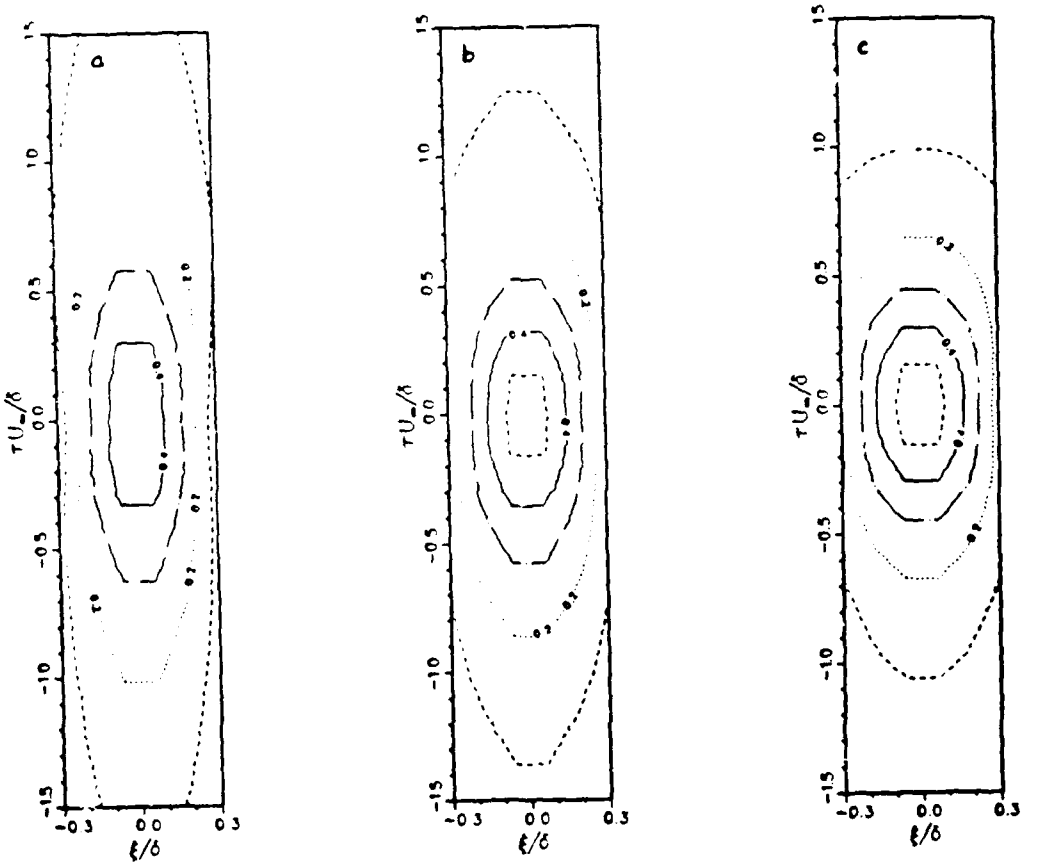

Fig. 15 Equi-value space-time correlation contours from spanwise separated velocity signals in the subsonic boundary layer studied by Alving. a) $y/\delta = 0.22$, b) $y/\delta = 0.52$, c) $y/\delta = 0.80$.

[illegible] boundary layer

shock wave

compression corner

[illegible] Image of the instantaneous density field for a shock wave boundary layer interaction produced by a compression corner. The view is cross-section normal to the wall, obtained by M. W. Smith using Rayleigh scattering. The flow is from right to left, the upstream freestream Mach number is 2.5, the incoming boundary layer has R_δ = 25,000, and the corner angle is [illegible]

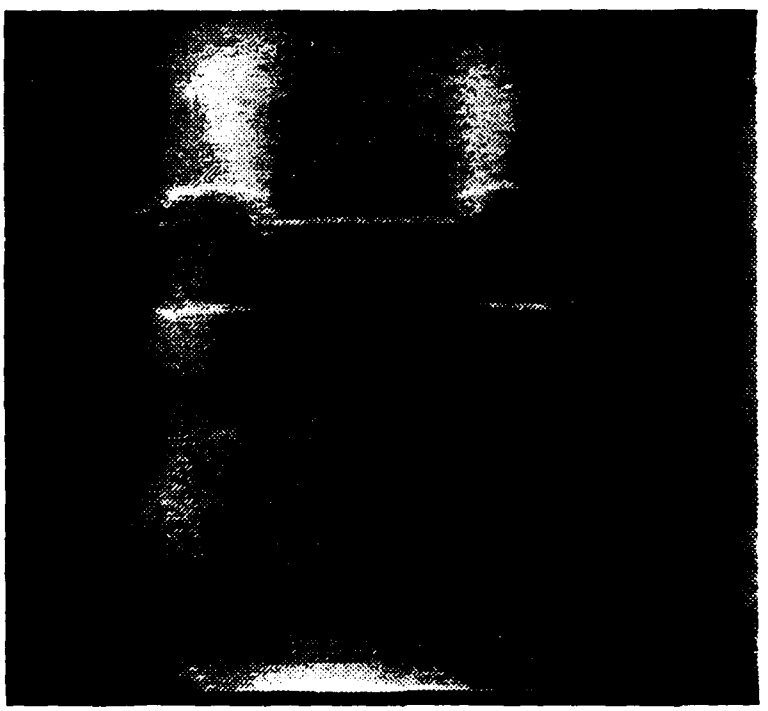

Figure 17 Cross-sectional image of density and line velocity profiles in an underexpanded air jet. Lines have been tagged before and after the Mach disk 2 μsec. before the image was recorded.

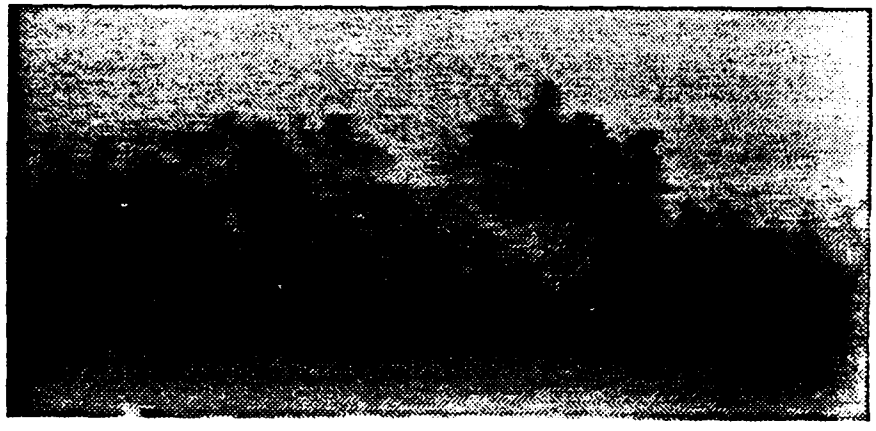

Figure 18 Density cross section across the boundary layer in a Mach 3.0 supersonic wind tunnel. Flow is from right to left.

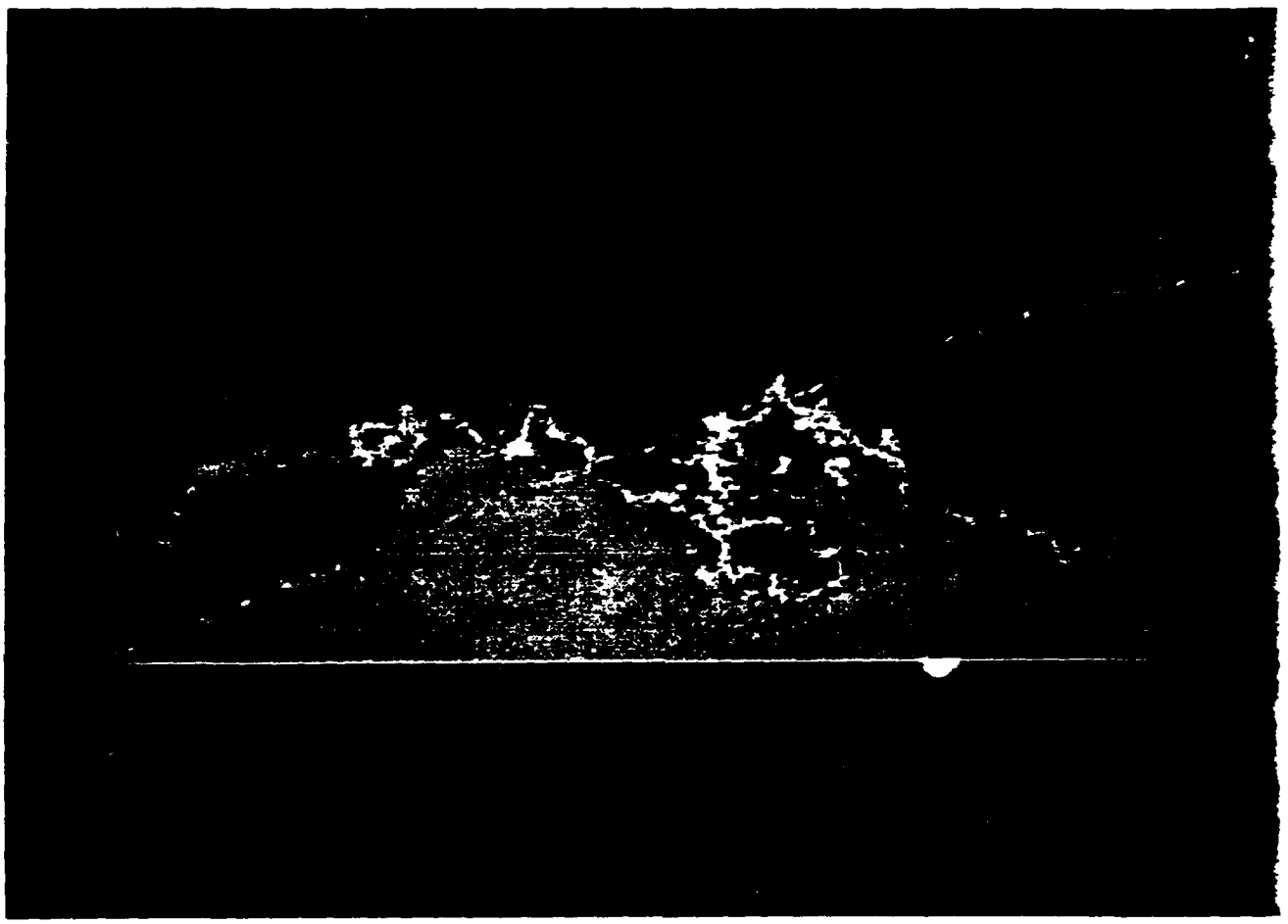

Figure 19 Color-enhanced image of the cross section across the boundary layer.

Figure 20 Density cross section parallel to the boundary layer at $y/\delta = .6$.

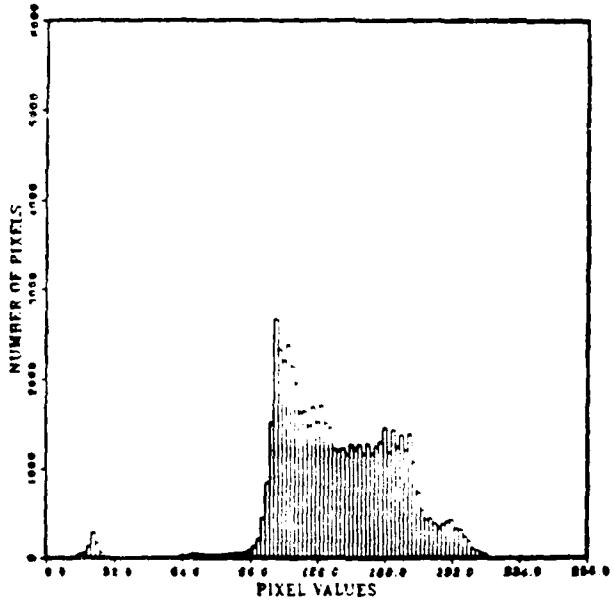

Fig. 21 Probability density function of the density at $y/\delta = .6$